

# Argonne National Laboratory

## THE STEADY STATE AND TRANSIENT KINETICS OF EBR-I, MARK-III

by

J. C. Carter, D. W. Sparks,

and

J. H. Tessier

## LEGAL NOTICE

*This report was prepared as an account of Government sponsored work. Neither the United States, nor the Commission, nor any person acting on behalf of the Commission:*

- A. Makes any warranty or representation, expressed or implied, with respect to the accuracy, completeness, or usefulness of the information contained in this report, or that the use of any information, apparatus, method, or process disclosed in this report may not infringe privately owned rights; or*
- B. Assumes any liabilities with respect to the use of, or for damages resulting from the use of any information, apparatus, method, or process disclosed in this report.*

*As used in the above, "person acting on behalf of the Commission" includes any employee or contractor of the Commission, or employee of such contractor, to the extent that such employee or contractor of the Commission, or employee of such contractor prepares, disseminates, or provides access to, any information pursuant to his employment or contract with the Commission, or his employment with such contractor.*

TABLE OF CONTENTS

ABSTRACT	ARGONNE NATIONAL LABORATORY	3
	9700 South Cass Avenue	
	Argonne, Illinois 60440	
I. INTRODUCTION		3
II. ORIGIN OF THE MODEL		4
III. THE MODEL		7
Reactor	THE STEADY STATE AND TRANSIENT	7
Neutron Kinetics	KINETICS OF EBR-I, MARK-III	8
	by	
IV. COMPARISON OF MODEL AND REACTOR RESPONSES		9
	J. C. Carter	
V. STABILITY		12
Power Equilibrium	Reactor Physics Division	12
Influence of Reactivity on Stability	and	14
VI. SUMMARY		15
REFERENCES	D. W. Sparks and J. H. Tessier	16
	Reactor Engineering Division	

March 1964

Operated by The University of Chicago  
under  
Contract W-31-109-eng-38  
with the  
U. S. Atomic Energy Commission







## TABLE OF CONTENTS

	<u>Page</u>
ABSTRACT . . . . .	3
I. INTRODUCTION . . . . .	3
II. ORIGIN OF THE MODEL . . . . .	4
III. THE MODEL . . . . .	7
Restrained Fuel Motion . . . . .	7
Neutron Kinetics, Thermal, Elasticity . . . . .	8
IV. COMPARISON OF MODEL AND REACTOR RESPONSES . . . .	9
V. STABILITY . . . . .	12
Power Equilibrium . . . . .	12
Influence of Reactivity on Stability . . . . .	14
VI. SUMMARY . . . . .	15
REFERENCES . . . . .	16



## LIST OF FIGURES

<u>No.</u>	<u>Title</u>	<u>Page</u>
1.	Reactor Block Diagram . . . . .	4
2.	Feedback Amplitude Ratio Versus Frequency . . . . .	5
3.	Feedback Phase Versus Frequency . . . . .	6
4.	Reactivity Loss Versus Power . . . . .	6
5.	Restrained Motion of a Fuel Rod . . . . .	7
6.	Block Diagram and Equations Summary for One Axial Segment of a Fuel Rod . . . . .	9
7.	Amplitude Ratio of Closed-loop Describing Function . . . . .	10
8.	Phase of Closed-loop Describing Function . . . . .	11
9.	Describing Function of Restrained Thermal Expansion of the Core . . . . .	13
10.	Open-loop Describing Function Versus Frequency . . . . .	14
11.	Reactor Root-locus Family . . . . .	15

ditions is assessed through the interpretation of test data and through consideration of the describing function for the nonlinear thermal expansion. The influence of positive reactivity on stability is seen from the reactor root-locus family, which shows the location of the dominant complex roots of the incremental linearized system function for various values of reactivity and power.

## I. INTRODUCTION

This report summarizes the results of an investigation of the dynamic characteristics of EBR-II, MARK-III. The core and blanket blanket of this reactor consist of a vertical bundle of cylindrical tubes arranged about a concentric steel shell. The rods are separated from each other and from the steel shell by radial spacers, thus permitting NaK to flow through the bundle parallel to the longitudinal axis of the core. Flow of the NaK coolant through the blanket and core may be in series or in parallel during any test, and the NaK inlet temperature and velocity through the tube bundle may be varied.





# THE STEADY STATE AND TRANSIENT KINETICS OF EBR-I, MARK-III

by

J. C. Carter, D. W. Sparks

and

J. H. Tessier

## ABSTRACT

The dynamic behavior of EBR-I, MARK-III, is examined to explain the dynamic behavior of the major inherent reactivity feedback sources in this fast reactor. The analysis begins with the reduction of measured test data, which shows that the feedback function contains a significant nonlinearity.

From consideration of structural features of the reactor, it is postulated that the observed nonlinearity arises from the restraint imposed on the free thermal expansion of the core by frictional forces between adjacent fuel rods. A mathematical model of the restrained thermal expansion is presented, and model and reactor responses are compared.

Stability of the reactor under power equilibrium conditions is assessed through linear extrapolation of test data and through consideration of the describing function for the nonlinear thermal expansion. The influence of positive reactivity on stability is examined through use of a root-locus family, which shows the location of the dominant complex roots of the incremental linear-equivalent system function for various values of excess reactivity and power.

## I. INTRODUCTION

This report summarizes the results of an investigation of the dynamic characteristics of EBR-I, MARK-III. The core and concentric blanket of this reactor consist of a vertical bundle of zirconium-clad uranium rods in a concentric steel shell. The rods are separated from each other and from the steel shell by radial spacers, thus permitting NaK to flow through the bundle parallel to the longitudinal axis of the core. Flow of the NaK coolant through the blanket and core may be in series or in parallel during any test, and the NaK inlet temperature and velocity through the tube bundle may be varied.





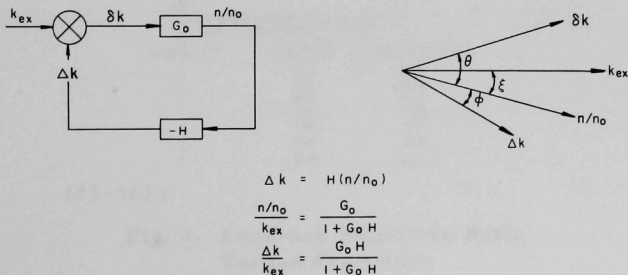
The major objectives of this study were: (1) to determine an analytical model of the important feedback-reactivity sources inherent in the reactor which is physically plausible and which results in agreement with measured test data; and (2) to examine the steady-state and transient behavior and stability of the reactor by using the derived model.

## II. ORIGIN OF THE MODEL

The model developed in these studies to describe EBR-I, MARK-III, behavior was derived from consideration of core-physics calculations which yielded reactivity coefficients for the sources of inherent reactivity compensation, and from a wealth of test data, particularly those obtained from reactivity oscillator tests.<sup>(1)</sup>

Static-physics calculations showed the two important sources of feedback reactivity to be: (1) changes in core and blanket dimensions; and (2) changes in the density of the coolant NaK. Other sources of inherent reactivity compensation were found to be negligible in comparison. Since changes in core and blanket dimensions and NaK density are essentially only temperature-dependent in this reactor, it seemed reasonable to expect that a model employing appropriate characterization of the neutronic and thermal dynamics would yield results in acceptable agreement with test data. However, we (and other investigators) soon discovered that such agreement did not exist and, in particular, that the reactivity-feedback transfer function computed from oscillator test data exhibited more amplitude attenuation and phase shift than could reasonably be attributed to the thermal model and to normally associated thermal expansion.<sup>(2,3)</sup>

Figure 1 illustrates, in simple form, a block diagram representation of the reactor. Here  $G_0$  is the neutron kinetics or zero-power transfer function, and  $H$  is the total-feedback function. Oscillator test data consists of measured values of the amplitude and phase of  $n/n_0$  in response to sinusoidal



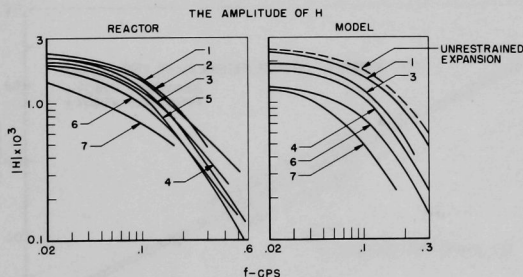
111-8302

Fig. 1. Reactor Block Diagram



variations of the excess reactivity input,  $k_{ex}$ . To determine  $H$  from the test results, the net input reactivity  $\delta k$  is computed first through use of the known function  $G_0$ . Then the vector subtraction of  $\delta k$  and  $k_{ex}$  is performed to yield the amplitude and phase of the feedback reactivity  $\Delta k$ . Then  $H$  is computed as the ratio,  $\Delta k/(n/n_0)$ .

In Fig. 2 the curves on the left depict sample results of such calculations. Here the amplitude of  $H$  is shown as a function of frequency for various power levels, and with two different values of the worth of the oscillator rod. These amplitude curves have been power-normalized by multiplying each by the ratio: 1150 kW/actual test power. The spread in this family of curves is evidence of another feature of the feedback function which is not explained by the thermal model alone; viz., a significant non-linearity exists in  $H$ . Since, for this set of curves, the NaK flow rate is constant, the thermal equations are essentially linear, and power-normalized amplitude curves derived therefrom would all coincide with the dashed curve shown in the set on the right, labeled "unrestrained expansion." Note that the true amplitude of  $H$  is less than that predicted by the linear thermal model, the effect generally increasing as power decreases. The corresponding phase curves shown in Fig. 3 also exhibit a spread in values, the tendency being to develop more phase lag as power is decreased.



#### NOTES

1-  $H$  NORMALIZED TO  $H$  AT 1150 KW  
2- NaK FLOW-300 GPM (SERIES)

CURVE NO.	POWER-KW	OSCILLATOR ROD
1	1150	NEW
2	952	NEW
3	877	OLD
4	877	NEW
5	655	OLD
6	489	OLD
7	370	OLD

111-7620

Fig. 2. Feedback Amplitude Ratio  
Versus Frequency

Additional evidence of the nonlinearity in  $H$  was obtained by examining measured values of reactivity loss versus reactor power level. Figure 4





indicates that the reactivity-power relationship follows different curves for increasing and decreasing power, resulting in a form of hysteresis loop. This, of course, would not occur if the feedback were truly linear.

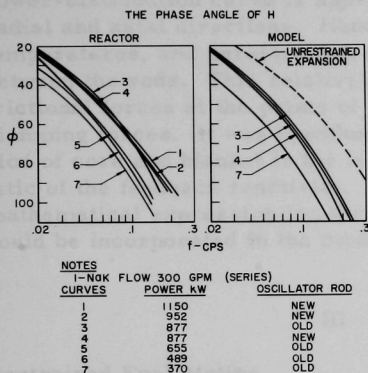
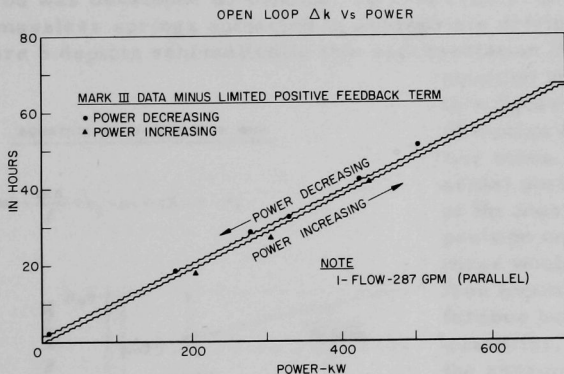


Fig. 3  
Feedback Phase Versus Frequency

111-7621



111-8080

Fig. 4. Reactivity Loss Versus Power

Thus a major problem in the analysis of MARK-III behavior was to determine a physically plausible nonlinear mechanism which acts to modify the feedback reactivity in the manner indicated by test results. Attention was then directed to a detailed examination of the structural design of the core in search of such a mechanism. It became apparent that considerable interference to the thermal expansion of the core and blanket could exist. During assembly, the reactor core and blanket are subjected to manual circumferential clamping which presses the bundle of fuel rods into radial

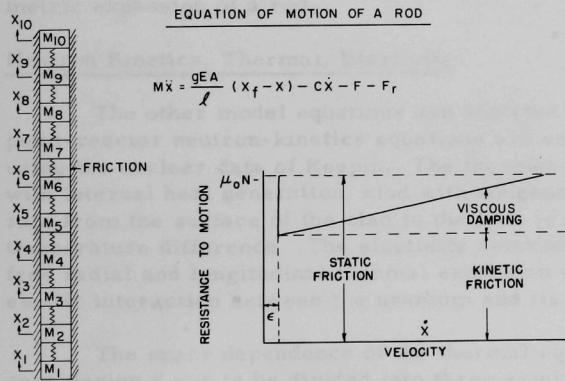


contact. These pressures are supported by the steel reactor shell. As the reactor is brought up to power, the hot core region tends to expand. But the radial expansion is inhibited by the restraining action of the relatively cool shell, and thus the clamping forces increase. The shape of the core power-distribution curve is approximately a chopped cosine in both the radial and axial directions. Hence, adjacent fuel rods will be at different temperatures, and unrestrained expansion would involve relative motion between the rods. This relative motion is restrained, however, due to the frictional forces at the points of contact between the rods developed by the clamping forces. It was hypothesized that this restraint to the free expansion of core and blanket is the major contributor to the nonlinear characteristic of the feedback reactivity. To test this hypothesis, an appropriate mathematical expression for the restrained rod motion was developed which could be incorporated in the model of the total MARK-III system.

### III. THE MODEL

#### Restrained Fuel Motion

The differential equation describing the restrained longitudinal motion of a rod was developed by considering it to consist of a set of lumped masses and massless springs subjected to appropriate driving and damping forces. Figure 5 depicts schematically this representation of a rod. The



111-8300

Fig. 5. Restrained Motion of a Fuel Rod

restraint friction terms which represent respectively, viscous friction, kinetic or sliding friction, and static friction. The action of these frictional

equation shown in this figure is the equation of motion of a representative mass. Here,  $x$  is the actual position coordinate of the mass, and  $x_f$  is the position coordinate the mass would have under free expansion. The difference between these two quantities, multiplied by the appropriate elasticity modulus for the rod, forms the thermal expansion force which is the model spring force and constitutes the first term on the right side of the equation. The other terms on the right side of this equation constitute the motion-





forces is considered to depend on the velocity of the mass as depicted in the graph of Fig. 5. When the velocity of the mass is less than a very small value  $\epsilon$ , the only frictional force acting is  $F_r = \mu_0 N$ . When the mass velocity exceeds  $\epsilon$ , the static-friction term becomes zero, and the mass then moves in opposition to the combined frictional forces,  $c\dot{x}$  and  $F$ , as shown.

Motion of the mass begins when the expansion force becomes equal to the force of static friction. The average velocity of the moving mass is very great and is in particular much greater than  $\dot{x}_f$ . Therefore, as the mass moves in opposition to the kinetic and viscous friction forces, the expansion force diminishes, and when the velocity of the mass becomes zero, the mass again comes under the influence of the static friction force. The expansive force again begins to build up, and the cycle repeats itself so that the restrained motion of the mass occurs in a series of steps or jumps. Details of the motion of the mass are determined by assigning values to the friction coefficients contained in the equation of motion.

The radial expansion of the core and blanket is inhibited by the forces necessary for elastic deformation of the hex cans containing the rods. Frictional forces again arise due to relative motion between adjacent rods. Hence it is assumed that the friction-restraint mechanism described above for longitudinal expansion also applies to radial expansion. It is assumed that the unit-free radial expansion is equal to the unit-free longitudinal expansion, and that the volumetric expansion is three times either of these. The model equation of friction-restrained motion was then applied to the volumetric expansion of a rod.

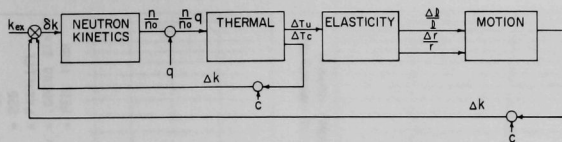
### Neutron Kinetics, Thermal, Elasticity

The other model equations are depicted in Fig. 6. Conventional, point-reactor neutron-kinetics equations are employed with six delay groups using the nuclear data of Keepin. The thermal equations are for a cylinder with internal heat generation, clad with nongenerating material. Heat-flow rate from the surface of the clad to the NaK is determined by the log-mean temperature difference. The elasticity relationships yield the values of unit-free radial and longitudinal thermal expansion of a rod, accounting for the elastic interaction between the uranium and its zirconium clad.

The space dependence of the thermal equations was eliminated by considering a rod to be divided into three axial and three radial sections, resulting in a set of ordinary differential equations representing average conditions in each element.

The intercoupling of these equations is indicated by the block diagram representation at the top of Fig. 6.





EQUATIONS ASSOCIATED WITH ONE AXIAL SEGMENT OF A ROD

NEUTRON KINETICS

$$\frac{dn}{dt} = \frac{k_{\text{ex}}(1-\beta) - \beta n}{\lambda_1 C_1} + \sum_{i=1}^6 \lambda_i C_i$$

$$\frac{dc_i}{dt} = \frac{(1+k_{\text{ex}})\beta_i n}{\lambda_i C_i} - \lambda_i C_i$$

TEMPERATURE DISTRIBUTION

$$\text{cpp} \frac{\partial^2 T(r,t)}{\partial r^2} = k_u \left( \frac{\partial^2 T(r,t)}{\partial r^2} + \frac{\partial T(r,t)}{\partial r} \right) + \frac{n}{n_0} q$$

$$\text{cpp} \frac{\partial^2 T_z(r,t)}{\partial r^2} = k_z \left( \frac{\partial^2 T_z(r,t)}{\partial r^2} + \frac{\partial T_z(r,t)}{\partial r} \right)$$

$$q = h s \frac{(T_z - T_c) - (T_{z2} - T_{c2})}{\ln \left( \frac{T_z - T_{c2}}{T_{z2} - T_c} \right)}$$

ELASTICITY

$$V_u = V_z$$

$$V_u = 2\pi \int_0^R V(r) r dr \quad V_z = 2\pi \int_0^c V(r) r dr$$

$$V = \frac{1}{2E} (\sigma_r^2 + \sigma_z^2) - \frac{\nu}{E} \sigma_r \sigma_z + \frac{1-\nu}{E} \tau^2(r,t)$$

$$\left( \frac{\Delta L}{L} \right)_u = \frac{q \Delta T - \delta}{A}$$

$$\left( \frac{\Delta L}{L} \right)_z = \frac{A(q \Delta T_1 - \delta - B q \Delta T_2)}{A + B}$$

$$\frac{\Delta L}{L} = \frac{(A q \Delta T_1)_u + (A q \Delta T_2)_z}{(A E)_u + (A E)_z}$$

MOTION OF ROD

$$m \frac{d^2 x}{dt^2} = \frac{QEA}{L} (x_1 - x) - c \frac{dx}{dt} - F - F_r$$

$$F_r = \mu_0 N$$

$$F = \mu_0 N (F_c + c F \frac{dx}{dt})$$

$$\text{FOR } 0 < x < \xi \quad F_r = \mu_0 N \quad F = 0 \quad Cx = 0$$

$$\text{FOR } x > \xi \quad F_r = 0 \quad \Sigma \text{ force} = F + Cx$$

111-8364

Fig. 6. Block Diagram and Equations Summary  
for One Axial Segment of a Fuel Rod

These equations were applied to one core and one blanket fuel rod, each representing average power conditions for its region. The resulting sets of equations were programmed for and solved by an analog computer. The analog simulation of the MARK-III model was then used to determine the appropriate values of the constants to be used in the nonlinear equation of motion of the rods. These constants were selected to yield the best fit of model responses to a specific set of MARK-III data, and once selected were held constant for all subsequent reactor operating conditions.

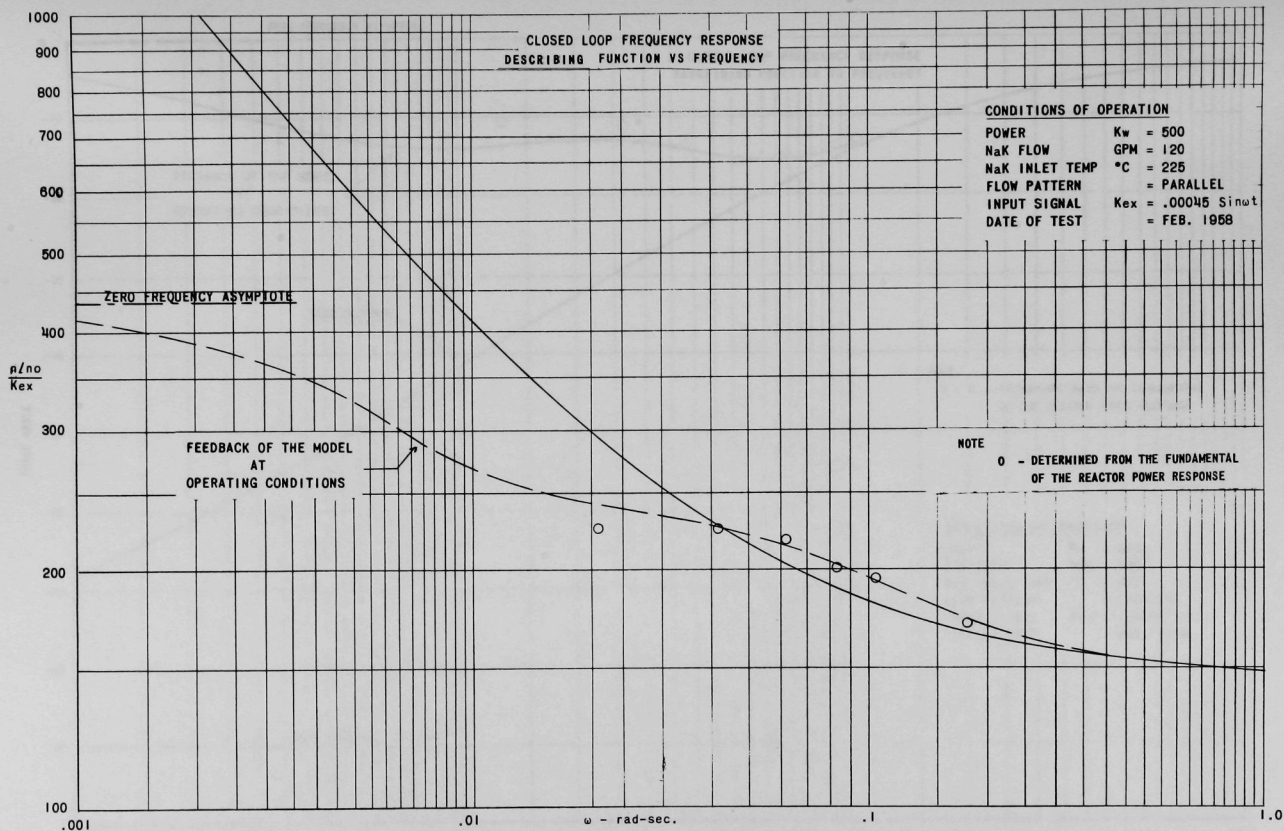
#### IV. COMPARISON OF MODEL AND REACTOR RESPONSES

The model and the measured reactor responses compared favorably for a wide variety of operating condition.

Comparison of the model and reactor closed-loop describing function is shown in Figs. 7 and 8 which depict, respectively, the amplitude and phase of  $(\Delta n/n_0)/k_{\text{ex}}$ . The circled points are the test-data values of these quantities. The approach to zero-power curves at high frequency is depicted.

Figures 2 and 3 indicate the agreement between the model and the measured values of the total feedback function  $H$ . Here the curves on the right represent the values of the amplitude and phase of  $H$ , as determined from measurement on the analog model. Comparison of these curves with those for the reactor on the left of these figures shows the agreement to be quite good both in trend and in quantitative values.



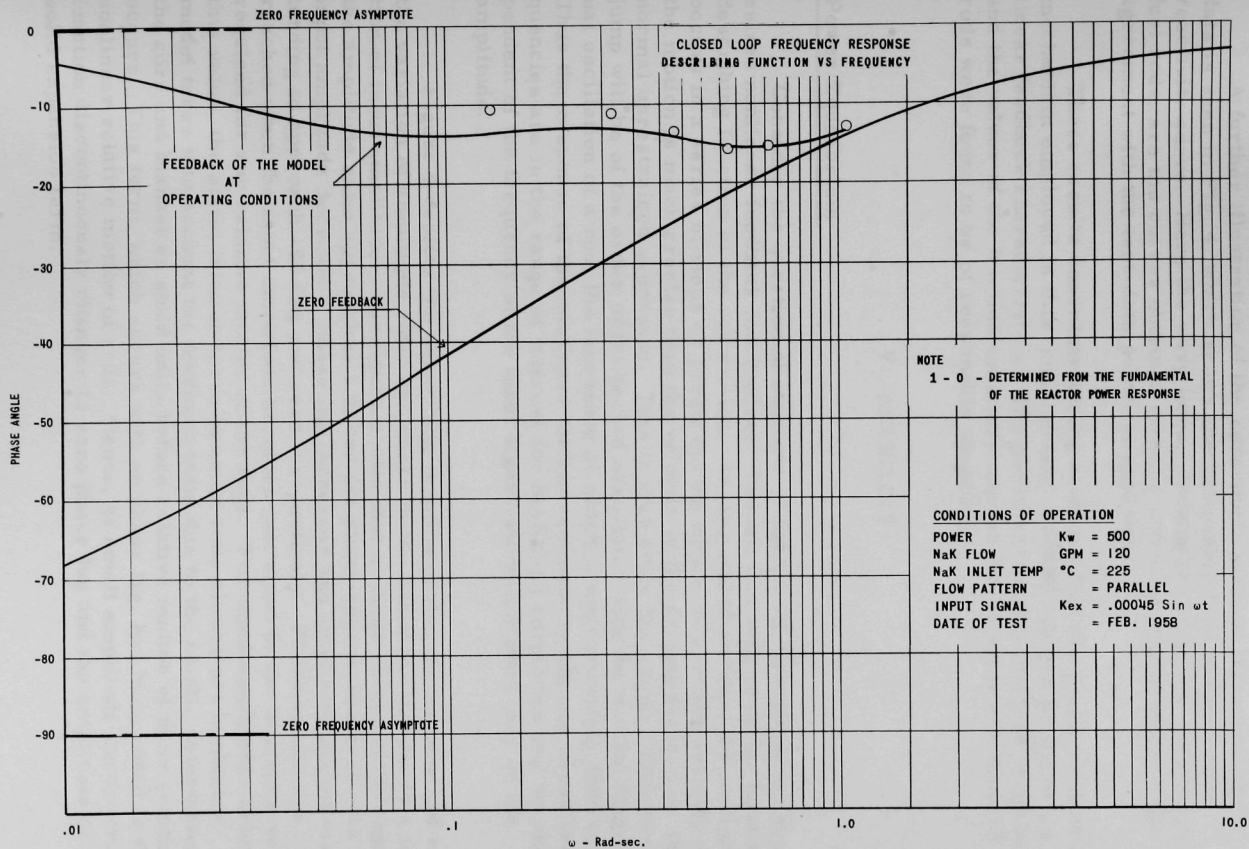


111-8545

Fig. 7. Amplitude Ratio of Closed-loop Describing Function







111-8544

Fig. 8. Phase of Closed-loop Describing Function



A further illustration of the agreement between the model and test data is seen in Fig. 4, which shows the hysteresis loop in the power-reactivity curve. Here the wavy lines, showing the step-like motion of the fuel rods, are the curves obtained directly from the analog model. The agreement with the test-data points is apparent.

These results constitute strong evidence that the nonlinear feedback mechanism employed in this model exists in MARK-III and produces its nonlinear feedback characteristics. The physical process involved is plausible and the values of the friction constants used in the equation of motion of the rods were found to be of reasonable magnitude.

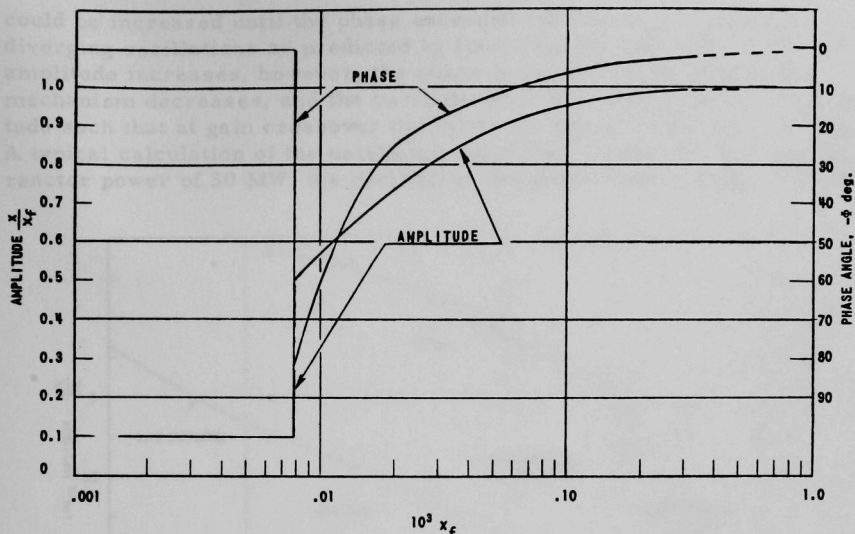
## V. STABILITY

### Power Equilibrium

Consider the question of stability of MARK-III, in light of the hypothesized nonlinear feedback mechanism. Toward this end, consider first the describing function of the rod motion. As was stated earlier, the motion occurs in a series of steps or jumps during which the average velocity of the motion is much greater than the velocity of the driving force, i.e., the normal unrestrained expansion. This is true since the elapsed time of a jump will be of the order of the period associated with the natural longitudinal oscillation of a rod, the frequency of which is approximately 4000 cps. Thus the response of the nonlinear motion equations to signals whose frequencies are in the range of interest for MARK-III responses will be independent of the frequency of the input signal and will depend only on the amplitude.

Figure 9 depicts the describing function of this mechanism and shows the variation of amplitude ratio and phase of the nonlinear motion as a function of input amplitude. The figure shows that at large values of the input, the amplitude ratio approaches 1.0, and the phase approaches zero. As the input amplitude decreases, phase lag increases and amplitude decreases, tending to approach -90 deg and zero, respectively. These values are reached when the input amplitude becomes just equal to the minimum value required for any relative motion of the rods. For input amplitudes below this value, the static friction force between rods always predominates. The model takes into account the feedback term due to the elastic deformation of the core and blanket as solid units before relative motion of their components occurs. This term, which occurs with no phase lag, has been added to the nonlinear relative motion of rods. Hence, at small amplitude the describing function discontinuously changes to zero phase lag and the amplitude of the solid expansion term.





111-9327

Fig. 9. Describing Function of Restrained Thermal Expansion of the Core

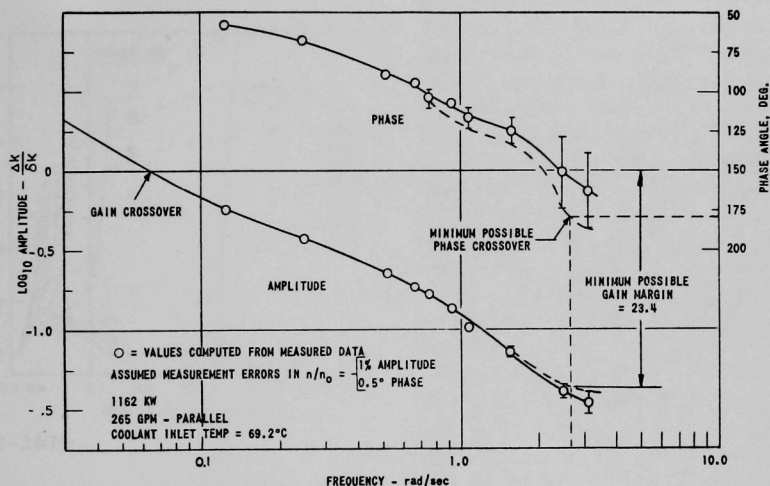
The application of normal linear-stability theory using this describing function leads to the conclusion that the reactor will be stable under any condition of operation which does not result in melting of core materials. To illustrate this, consider the reactor-open loop-describing function depicted in Fig. 10 of the available MARK-III data. The set from which the Bode plot of Fig. 10 was made represents the condition closest to instability. Error bands shown about the data points indicate the maximum errors which would result if the assumed errors in measurement of  $n/n_0$  were present. Thus the maximum phase lag is represented by the dashed curve connecting the lower error limits of the phase curve. As can be seen, the phase reaches the critical value of 180 deg at approximately 2.6 radians. At this point, the minimum gain margin (as defined by the upper error limits of the amplitude curve) is the factor 23.4. Hence, if the feedback mechanism were linear, the Bode plot predicts that the reactor power could be increased by a factor of 23.4 before instability would result. This, however, would yield a power level of 27.2 MW, much above the power level for which fuel melting occurs. Thus it appears that by the most pessimistic linear interpretation of MARK-III data, a power level capable of causing instability cannot be reached.

If the effects of the nonlinear feedback mechanism are considered, the stability prediction provided is even more optimistic than the foregoing result provided by linear extrapolation only. If, for example, reactor power





could be increased until the phase exceeded 180 deg at gain crossover, diverging oscillations as predicted by linear theory would begin. As the amplitude increases, however, the phase lag of the nonlinear feedback mechanism decreases, and the oscillatory motion would settle at an amplitude such that at gain crossover the total loop phase would equal 180 deg. A typical calculation of the oscillation magnitude shows that for nominal reactor power of 30 MW, the oscillation amplitude would be only  $\pm 33$  kW.



111-9326

Fig. 10. Open-loop Describing Function Versus Frequency

Thus it is concluded that in EBR-I, there appears to be no possibility that damage will ever result from self-excited oscillations building up spontaneously from a condition of power equilibrium at any attainable power.

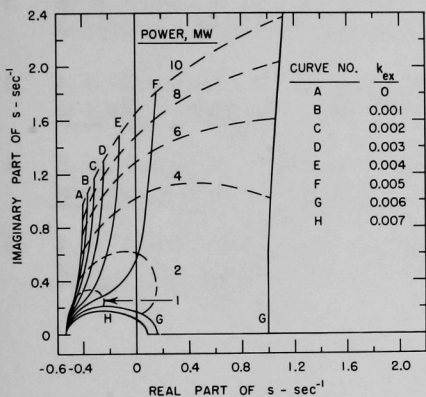
### Influence of Reactivity on Stability

The foregoing statements regarding the stability of EBR-I, MARK-III, have been based on the describing function as it exists for power equilibrium conditions of the reactor. During the analog studies with the MARK-III model, it was observed that a definite destabilizing influence existed when substantial amounts of positive reactivity were inserted. Our understanding of this effect remained qualitative until recently when we (and other workers) were able to develop analytical descriptions of the process involved. The history of these investigations and the results of work in this area were presented by D. W. Sparks in a paper entitled "The Period Effect in Reactor Dynamics."<sup>(4)</sup> As Sparks stated, the effect of positive reactivity in the kinetics-transfer function is to alter the gain and increase the phase lag,



these effects increasing rapidly as the prompt critical condition is approached. Thus a reactor appearing to be stable when examined through application of the normal zero-power transfer function may be quite unstable when positive reactivity is introduced.

The stability analysis of EBR-I, MARK-III, has been extended, therefore, to include the effects of positive reactivity. Figure 11 depicts a root-locus family showing the location of the dominant complex roots of the incremental linear equivalent to MARK-III for the values of  $k_{ex}$  and power indicated. This plot was developed using RE/290, a 704 code described in Reference 4, and a linearized fit to the total MARK-III feedback function. The destabilizing influence of positive reactivity is clearly evident in these curves as they shift toward the right-half S plane as  $k_{ex}$  increases. The great inherent stability of MARK-III is apparent, however, since there is no crossing of the imaginary axis for power levels up to and including 10 MW, or  $k_{ex}$  values up to approximately 0.0045 (66 cents). At design full power for the reactor (which is approximately 1 MW), the curves show the dominant complex roots to be well-damped



112-2679

Fig. 11. Reactor Root-locus Family

for values of  $k_{ex}$  exceeding the prompt critical value of 0.00683. This indicates that no sustained oscillations would result even when the reactor is placed on an extremely short period.

## VI. SUMMARY

In summary, the results of this analysis indicate the following:

1) From examination of the structural feature of EBR-I, MARK-III, it is believed that the restrained thermal-expansion model constitutes an explanation of the observed nonlinear feedback. The physical process and the constants in its defining equation seem plausible. The synthesized model of the reactor system yields good agreement with test data over a wide variety of operating conditions.

2) The feedback is such that EBR-I, MARK-III, has dynamic characteristics which cause it to be stable well beyond its operating range. This



conclusion applies (a) to stability assessments referred to operation about a point of power equilibrium, and (b) to stability assessment referred to nonequilibrium power conditions developed by the presence of positive reactivity.

#### REFERENCES

1. R. R. Smith, J. F. Boland, and F. W. Thalgott, Argonne National Laboratory (Private Communication).
2. J. C. Carter, D. W. Sparks, and J. H. Tessier, The Internal Feedback of EBR-I, MARK-III, ANL-6124 (Feb 1960).
3. R. R. Smith, J. F. Boland, F. D. McGinnis, M. Novick, and F. W. Thalgott, Instability Studies with EBR-I, MARK-III, ANL-6266 (Dec 1960).
4. J. C. Carter, D. W. Sparks, and J. H. Tessier, The Period Effect in Reactor Dynamics, ANL-6852 (April 1964).





ARGONNE NATIONAL LAB WEST



3 4444 00009146 2

X